RPN22

LABORATORY OF PLASMA STUDIES
CORNELL UNIVERSITY
ITHACA, NEW YORK

BEAM ENTRANCE CONDITION STUDIES

by

J. J. Clark

S. Linke

LPS 13

MAY 1969

This research was funded under Office of Naval Research (ONR) Contract No. N00014-67-A-0077-0003.

ABSTRACT

Observed operational characteristics of the high-field-emission diode of the Cornell Relativistic Electron Beam Accelerator are presented as functions of diode impedance over a range of cathode types, anode-cathode gap spacings, and vacuum pressures. Comparisons are made with expected predictions from the Child-Langmuir Law. Pin-hole, anode-plane radiographs are displayed, for a number of cathode designs, showing spatial current distribution and angular spread of electron trajectories. Preliminary studies of the time history of the current distribution in the anode-cathode gap are described. Results are presented in photographs obtained by fast-frame and time-integrated cameras.

A. TIME-INTEGRATED CURRENT DISTRIBUTION STUDIES

The Cornell field-emission diode, described in detail in reference [1], is shown in Figure 1 in schematic form. The "plasma" cathode depicted is a solid brass disk 4.0" in effective diameter by 5/8" thick with rounded edges. The emitting surface contains approximately 200 conical holes (1/4" diameter) filled with liquid lucite which has been allowed to harden. The surface has been faced off on a lathe and polished.

Diode voltage (V_D) is measured by means of a low-inductance carbon resistor voltage divider, and diode current (I_D) is measured by means of a $CuSO_4$ current shunt (see Figure 2). Typical V_D and I_D oscillograph traces are shown in Figures 3A, 3B.

Diode impedance (Z_D), measured during the flat resistive phase of the voltage and current waveforms, is seen in Figure 4* to be less than that expected from Child's Law predictions by a factor of approximately 2, over a broad range of anode-cathode gap spacings, and for pressures from 5×10^{-2} torr to 10^{-5} torr. Since the Cornell diode is normally operated at a pressure of 3×10^{-4} torr, this additional diode current is believed to be caused by beam generated ions** in the gap region. The ions partially neutralize the electronic space charge and allow more current than the hard-vacuum Child's Law prediction.

Since the propagation characteristics of the electron beam in the drift tube are largely determined by the spatial current distribution and angular spread of the electron trajectories at the anode plane, x-ray pinhole camera

---

* plotted as $Z_D\sqrt{V_D}$ vs S^2, where $Z_D\sqrt{V_D} = 4350\ S^2/A$
with V_D = Diode volts in tens of KV
Z_D = Diode impedance in ohms
A = Cathode area in square centimeters
S = Anode-cathode gap in centimeters.

** ions /cm/sec of beam travel $\simeq \frac{3.75 \times 10^{23}\ I\ p}{V}$ where I is in amperes, V is in volts, p is in torr.

measurements were made of the "plasma" cathode for a variety of input voltages, pressures and anode-cathode gaps. Most radiographs of the "plasma" cathode show a "honeycomb"-type emission pattern, the resolution of which indicates reasonably laminar flow, as was predicted by J. C. Martin of AWRE, United Kingdom, who originally suggested the "plasma"-cathode design. Figure 5, a rough sketch of the electric field lines in the anode-cathode gap region, shows $\overline{E}$ to be mainly composed of an E_z component and explains the flow laminarity. In contrast, needle cathodes, more commonly in use as high-current field emitters, generally have a fairly large E_R component [2], and as a result the electron stream is less laminar.

To attempt a better understanding of the observed radiograph patterns, shots were made on a "plasma" cathode whose conical holes were not filled with a dielectric. No change in overall diode impedance (Z_D) was observed for this unfilled case, but a distinctly different, less-regular emission pattern resulted. The contrast in the two types of emission patterns is perhaps best illustrated by a radiograph of a cathode in which half the holes were filled with lucite and half were left unfilled (see Figure 6). The dark center section of the radiograph is believed to be the result of a current "pinch"* in the anode-cathode gap. This compression occurs toward the end of the first V_D, I_D pulses and is dependent on diode current, voltage, and "aspect ratio"**. Z_D, measured for the half filled/half-unfilled case, was approximately the same as for the completely filled case.

Because Z_D remained invariant with the first three cathode designs used, it was decided to use cathodes of a quite different design in an effort to sort out the importance, if any, of such parameters as hole diameter, type of fill material, etc. Figure 7 shows some of the designs on which shots were made and

---

* "Pinch" is defined as a compression of the beam in the radial direction which occurs when the self-generated magnetic forces of the beam exceed the electrostatic repulsion forces.

** Defined as r_o/S where r_o = cathode radius (cm), S = anode-cathode gap (cm).

Table 1 orders the cathodes according to:

$$Z_D \propto \frac{1}{A} \text{ ; where A = total hole area}$$

$$Z_D \propto \frac{1}{C} \text{ ; where C = total hole circumference.}$$

Difficulty in comparing data on the various cathode types was encountered because the diode voltage (V_D) is controlled by the breakdown voltage of the pre-stabbed solid-dielectric blumlein switch for which the scatter was approximately ±6%. A substantial number of shots on each cathode design was therefore required in order to allow grouping of the shots with approximately constant input voltage to the diode. Table II contains early data on this ordering scheme with input voltage eliminated as a parameter and Z_D presented as a function of cathode design only. While promising, this procedure leads to no definite conclusion, since a comparison of Table II with Table I shows that the diode impedance orders according to either, 1/A or 1/C for a particular cathode.

A new switch fabrication technique has reduced the blumlein-switch scatter to ±2% and the data is more easily taken. Recent data (Table III) indicate that the cathode structures will order according to $Z_D \propto 1/A$ but additional data are required to firmly establish this conclusion.

The radiograph of the ridge cathode indicates that most of the emission is occuring over the lucite-filled region, the result being a "hollow" beam at the anode (see Figure 8). Calorimetry and angular divergence measurements are planned to determine how long the beam remains hollow. Such a beam allows more tractable mathematical analysis and presents the possibility of more efficient coupling for microwave diagnostic experiments, since a hollow beam does not have the disadvantage of self shielding the inner electrons from the microwave-coupling device.

B. TIME-DIFFERENTIATED CURRENT DISTRIBUTION STUDIES

Studies of the time history of the current distribution in the anode-cathode gap by means of fast frame (5, 10, 20 nsec.) and fast-streak photography have been initiated.

The masking technique used to decrease the primary beam current to a level compatible with a fast-rising (3 nsec.) scintillator material (pilot "B" scintillon) is shown in Figure 9. Electrons leaving the plasma-cathode surface pass through a 30% transmitting, 0.010" stainless steel mesh anode foil. The transmitted electrons next encounter 2 layers of 0.005" aluminum foil, 1 layer of 0.010" black drawing paper (used to absorb light reflected in the back direction and prevent it from reducing the overall resolution) and finally a 0.020" layer of scintillon. The calculated penetration depth of 300 KV electrons is 0.012" of aluminum, while the penetration depth of the x-rays produced by both the mesh and the aluminum sheets is a few centimeters. Since the electrons that reach the scintillon are more effective in producing optical photons in the scintillon than the x-rays which reach the scintillon (by a factor of at least 10^3), a scintillon thickness thin enough to pass the x-rays with little optical excitation allows one to discriminate against the x-rays, and, in effect, optically photograph the electron spatial distribution. Figure 10 is a time-integrated photograph made to test this idea. The black rectangle in the center of the photograph shows that there is no light output from the scintillon over a region where the aluminum mask thickness (0.015") exceeds the estimated electron penetration depth (i.e. 0.012" for 300 KV electrons). Were the scintillon being excited by x-rays from the stainless steel anode, etc. this effect would not be noticeable due to the much longer x-ray range in aluminum. The photograph therefore gives the spatial distribution of the electrons.

Figure 11 shows a time-integrated photograph and Figure 12 displays a 5 nsec./frame photograph of the plasma cathode for the following conditions:

$$V_D = 360 \text{ KV}$$

$$I_D = 61 \text{ KA}$$

$$Z_D = 5.9\Omega$$

Figure 13 shows the time-synchronized trace of V_D versus the framing camera marker pulses.

Work is now underway to improve the focus of the TRW framing camera, decrease the first frame "get away" time, and enlarge the image on the film by means of a telephoto-lens system. (For the same image-on-film size the framing/streak camera can be moved away from the electro-magnetic (or R-F) noise sources which affect the camera focus.) Simultaneously, the increased distance serves as an optical-delay line and effectively allows more time for the camera shutter to open.

C. FUTURE PLANS

1. The time-and-space-differentiated camera studies of the electron stream at the anode plane will be improved and extended to include fast-streak photographs under the conditions for which "pinching" in the diode occurs.
2. Measurements of the angular spread of the electrons at the anode will be made as a function of cathode geometry, by means of a modified "masking" technique plus scintillon and fast cameras.
3. Absolute measure of spatial-energy distribution of electrons at the anode will be made via distributed calorimetry.

D. REFERENCES

[1] ONR Radiation and High Altitude Project Annual Report, Lab. of Plasma Studies, Cornell Univ. (April 1968).

[2] J. L. Brewster, R. E. Anderson, J. L. Barbour, etal, "Feasibility of High-Voltage X-Ray Tubes as Intense Gamma and Neutron Sources," ~~Technical Report No. AFWL-TR-65-63, DDC, Alexandria, Virginia~~ Circuit and Electromagnetic System Design Note 9 (November 1965).

✓ corrections made
JB 2/21/73

TABLE I

DIODE-IMPEDANCE ORDER
FOR
VARIOUS CATHODE SURFACES
(BASED ON CATHODE GEOMETRY)

Z_D - ORDER	CATHODE - SURFACE TYPE	
LOW → HIGH	FOR $Z_D \propto \frac{1}{A}$:	FOR $Z_D \propto \frac{1}{C}$:
1	WIDE RIDGE	PLASMA*
2	PLASMA*	EDGE HOLES
3	MEDIUM RIDGE	CENTER HOLES
4	NARROW RIDGE	NARROW RIDGE
5	EDGE HOLES	MEDIUM RIDGE
6	CENTER HOLES	WIDE RIDGE
7	CROSS	CROSS
8	NON-UNIFORM HOLES	NON-UNIFORM HOLES

* MANY PLASTIC-FILLED HOLES OVER ENTIRE SURFACE

TABLE II

DIODE-IMPEDANCE ORDER
FOR
VARIOUS CATHODE TYPES
(EXPERIMENTAL RESULTS)

Z_D - ORDER LOW→HIGH	SHOT NUMBER	V_{MARX} (KV)	CATHODE TYPE	Z_D (OHMS)
1	13	246	SINTERED TUNGSTEN	5.65
2	6	246	PLASTIC-FILLED BRASS	6.35
3	9	246	UNFILLED BRASS	6.87
4	19	246	ALUMINUM WITH RIDGE	7.56
5	23	246	ALUMINUM WITH CROSS	8.00

TABLE III

DIODE-IMPEDANCE ORDER

PLASTIC-FILLED CATHODES ($Z_D \propto \frac{1}{A}$)

Z_D - ORDER LOW→HIGH	ANODE-CATHODE GAP IN MM.	RELATIVE V_{INPUT}	CATHODE TYPE	A* (SQ. INCHES)	Z_D OHMS (MEASURED)
1	8	1.0	PLASMA	9.69	5.44
2	8	1.0	NARROW RIDGE	2.98	8.02
3	8	1.0	NON-UNIFORM HOLES	0.5	13.8

* CALCULATED AREA OF SURFACES OF THE DIELECTRIC FILLER MATERIAL.

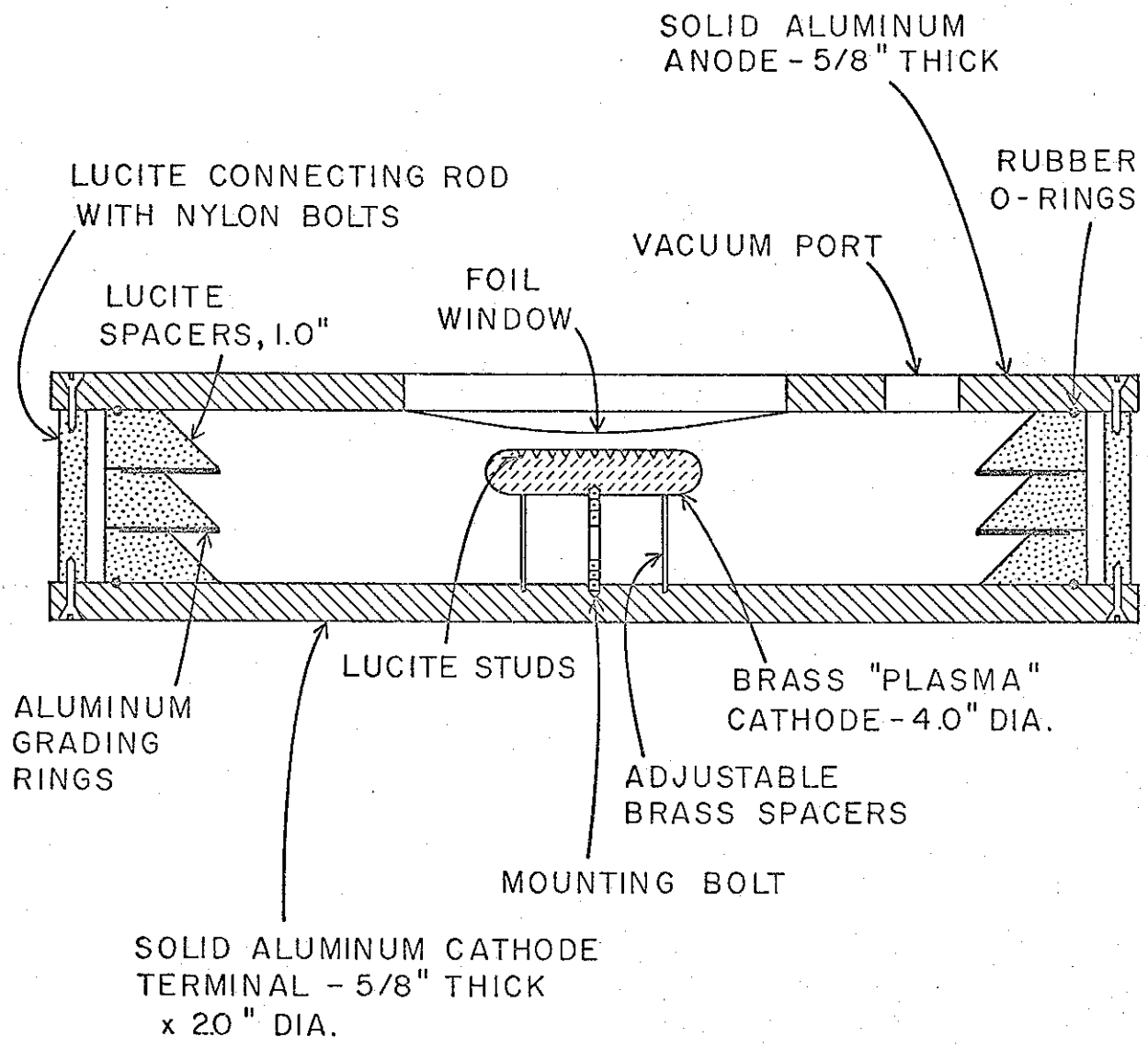

Fig. 1. Sketch of diode assembly (approximately 1/5 full size)

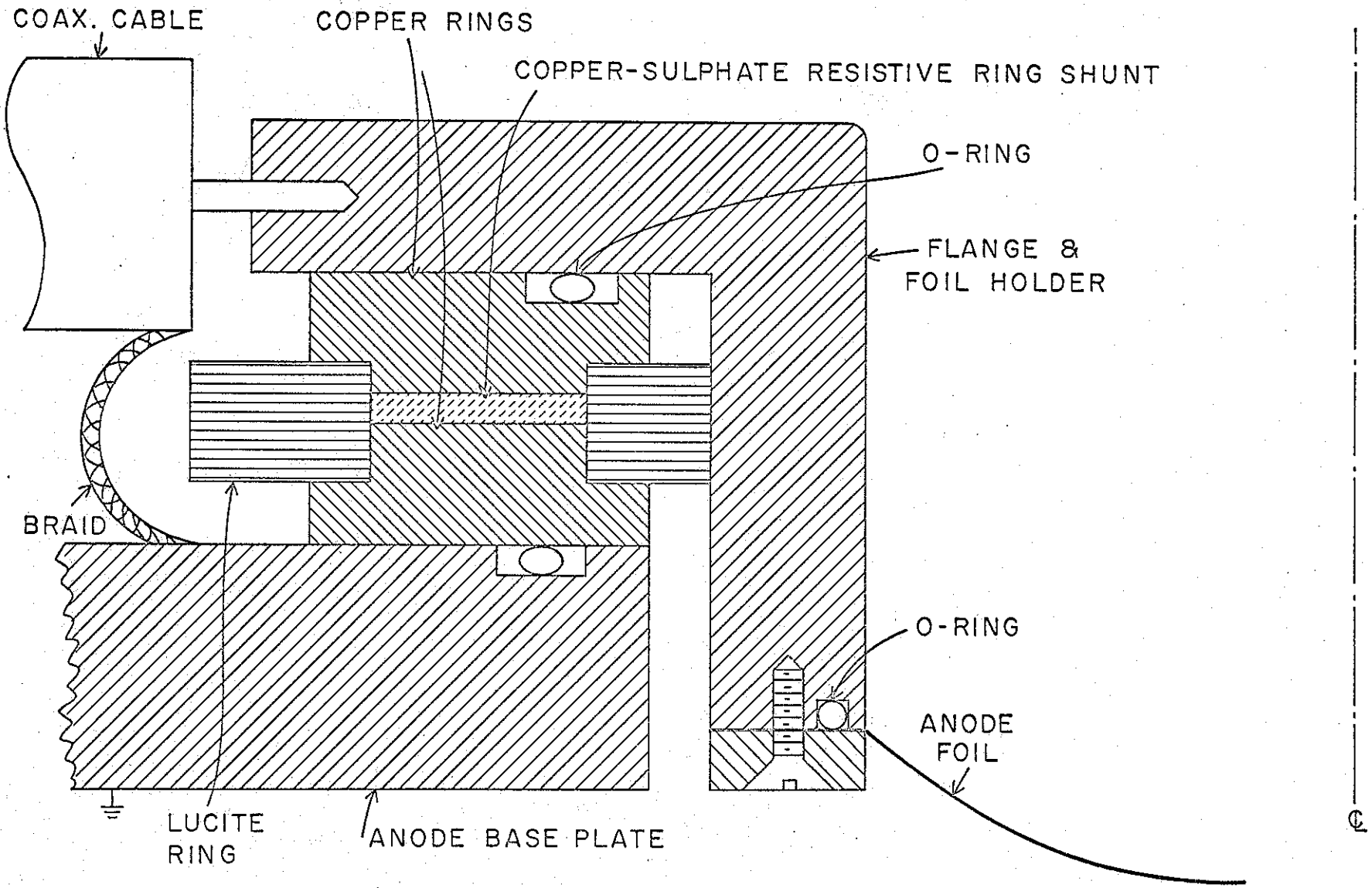

Fig. 2. Cross-section of current shunt and foil support
(scale: approximately three times actual size)

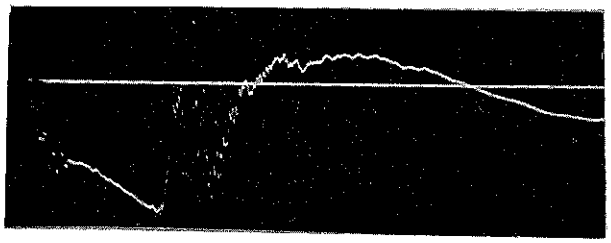

.5 microseconds/div

Marx Generator Voltage - Transmission line switch fires at sharp discontinuity.

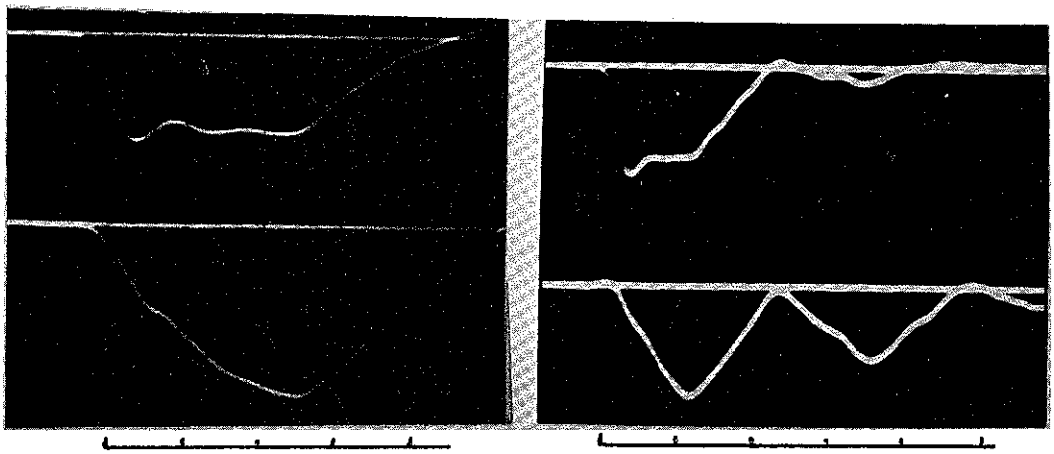

20 nanoseconds/div

V_D = 358 KV
I_{peak} = 76 KA
Z_D = 4.7 ohms
Shot # 5, 5/1/69

50 nanoseconds/div

V_D = 337 KV
I_{peak} = 50 KA
Z_D = 6.74 ohms
Shot # 11, 5/14/69

Figure 3 TYPICAL DIODE MONITOR WAVEFORMS

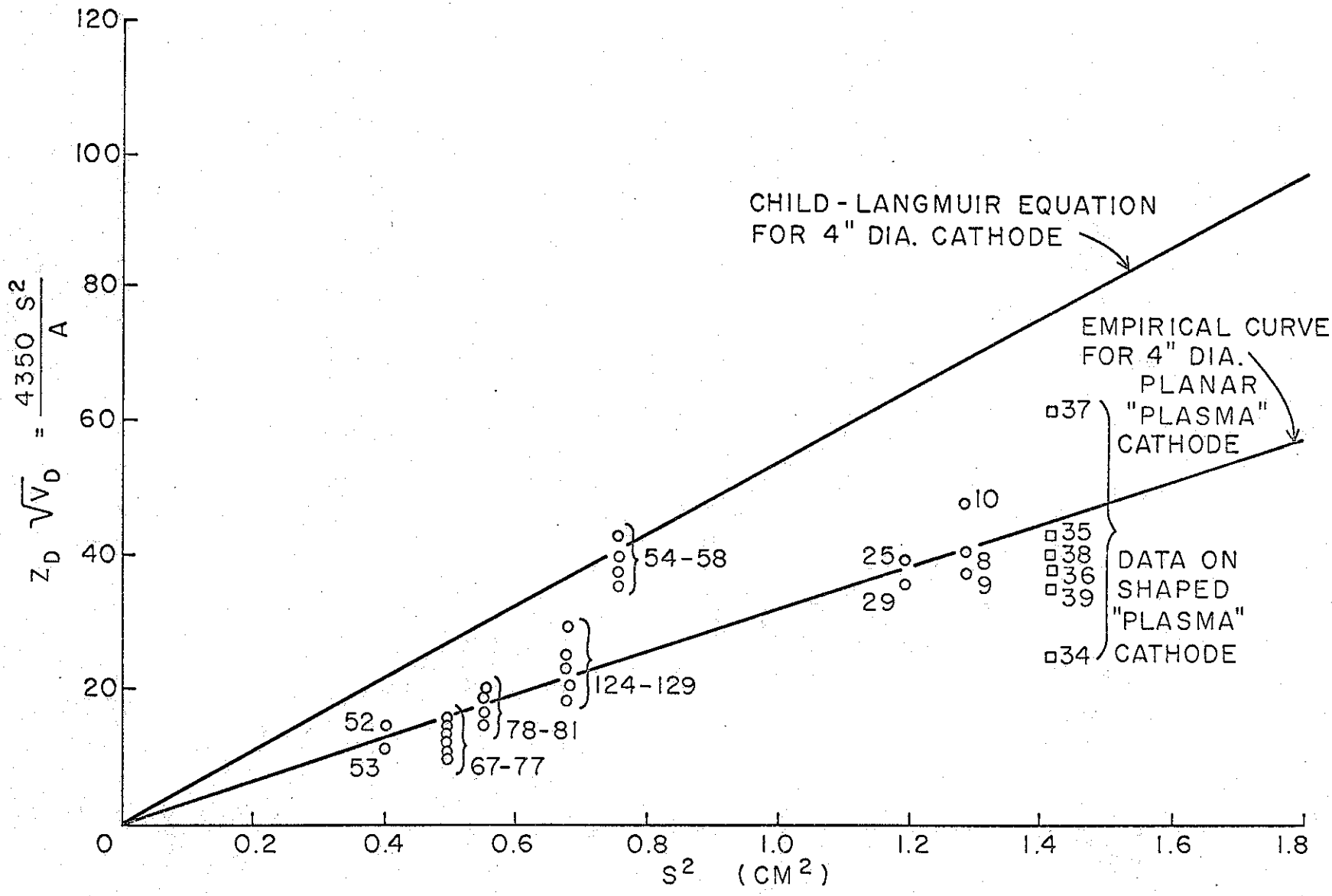

Fig. 4. Measured diode impedance compared to Child-Langmuir prediction

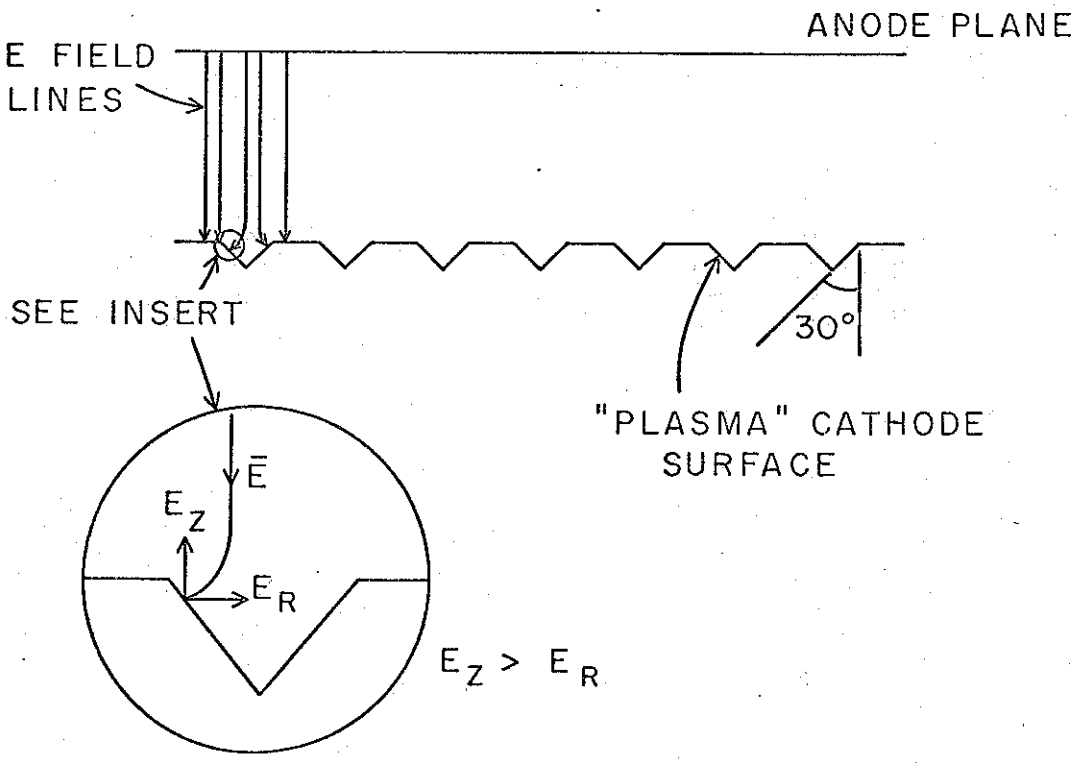

Fig. 5. Rough sketch of electric field lines in anode-cathode gap.

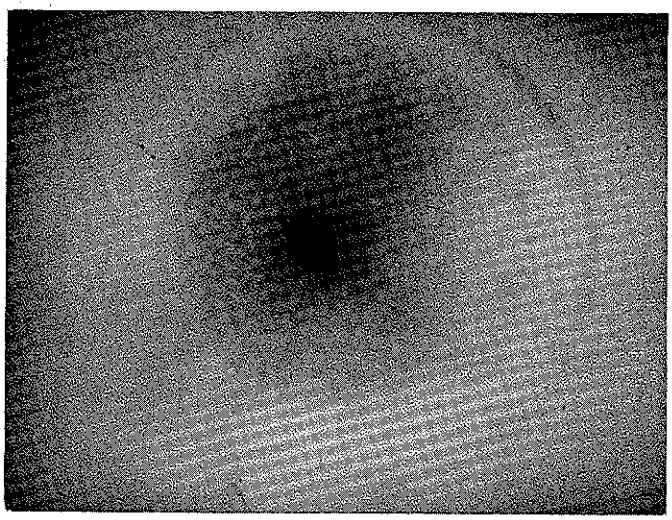

Fig. 6. Radiograph of half/half cathode (left half filled-right half unfilled) V_D = 379 KV, I_D = 58.5 KA, Z_D = 6.48 Ω
Shot #3, 10/30/68

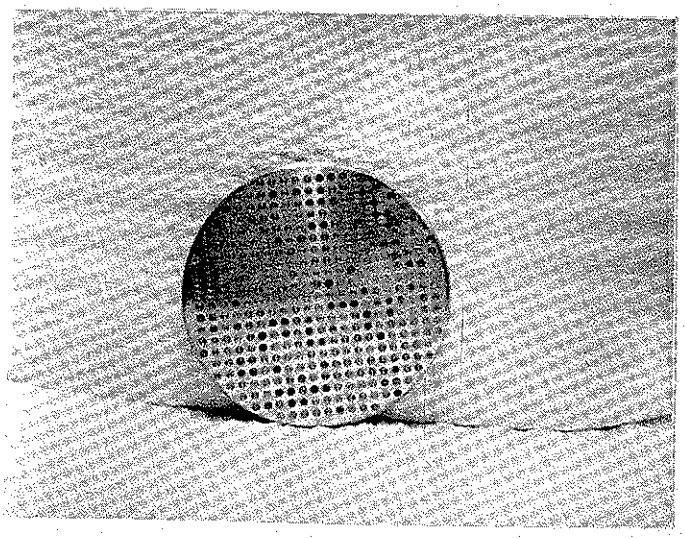

Fig. 7. "Plasma" cathode (filled)
(After 35 shots)

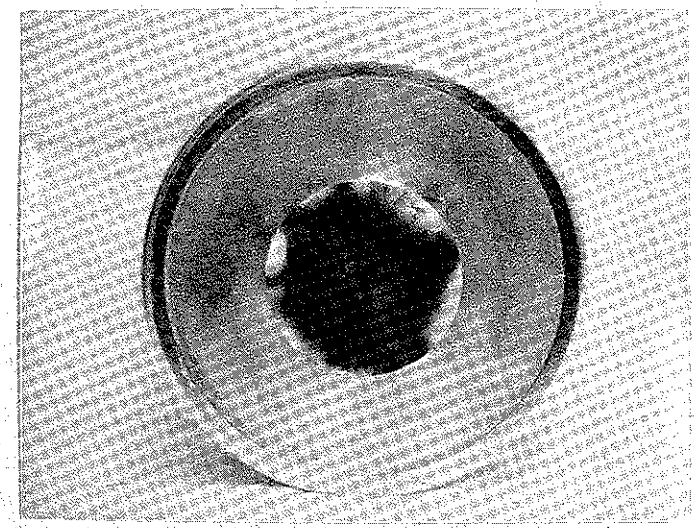

Wide ridge cathode (filled)
(After 10 shots)

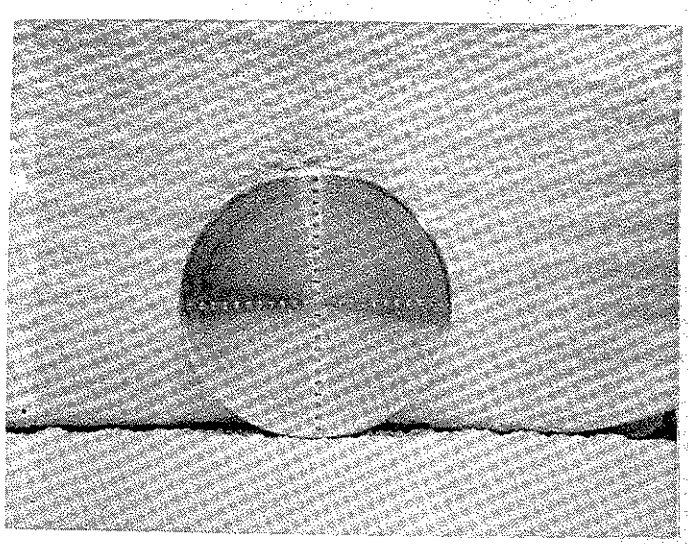

Cross cathode

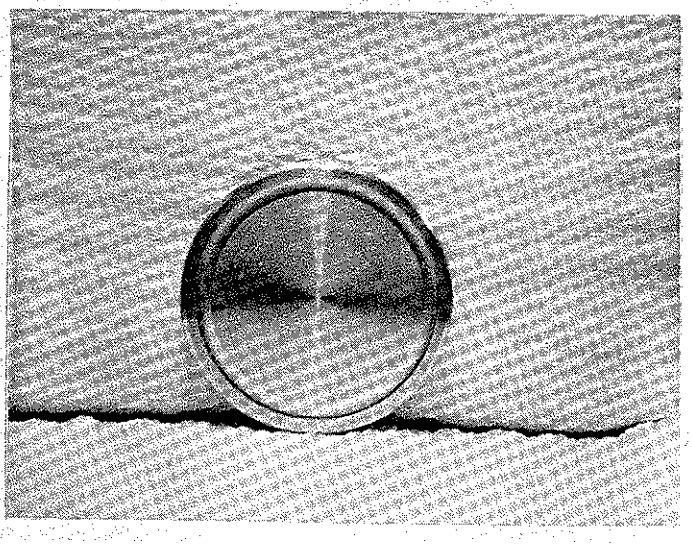

Narrow ridge cathode (unfilled)

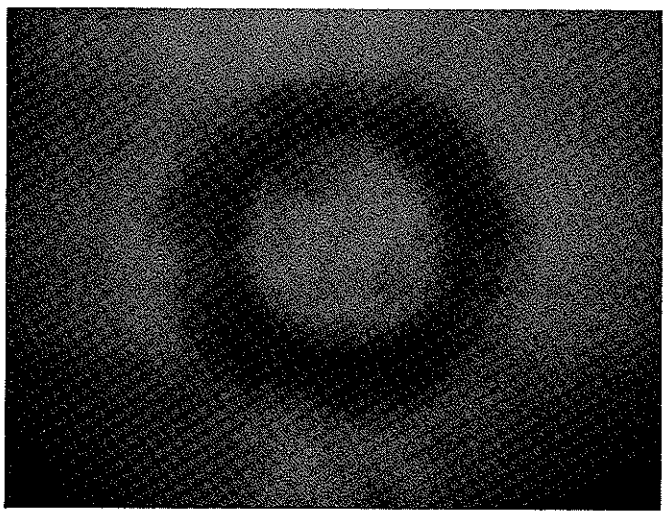

Fig. 8. Radiograph of ridge cathode
V_D = 373 KV, I_D = 47.3 KA, Z_D = 7.88 Ω
Shot #5, 10/30/68

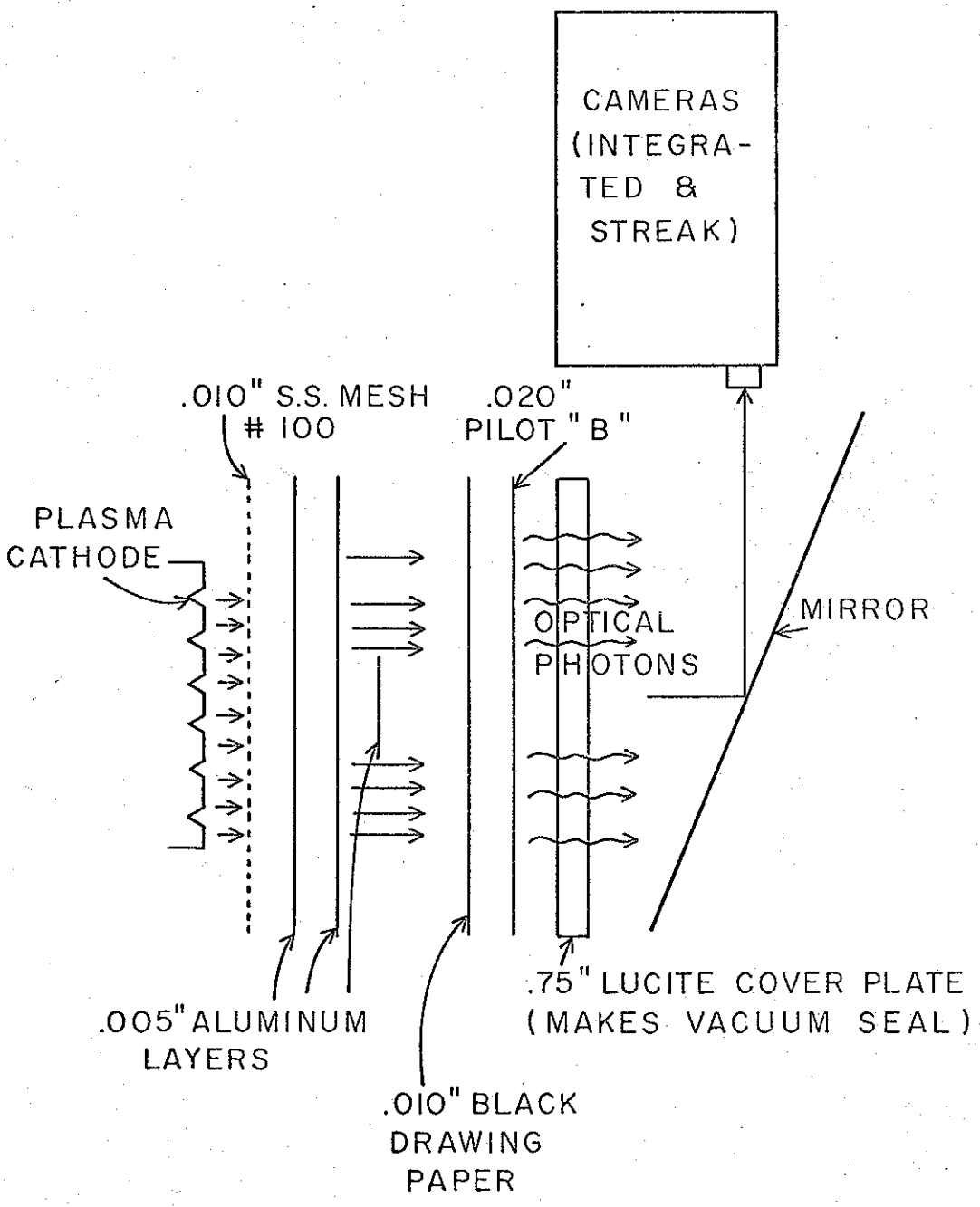

Figure 9. Masking Technique for Time-Differentiated Electron-Beam Studies

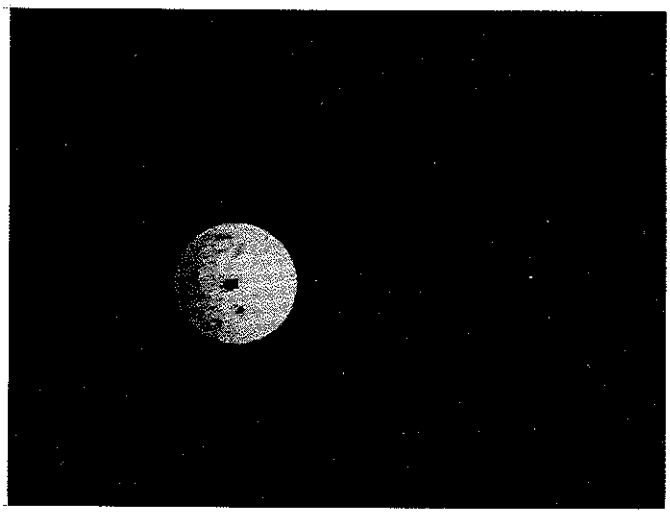

Fig. 10. Time-integrated photograph illustrating electron spatial distribution.
Polaroid film - type 47, f/32 + neutral density filter (x 10)
V_D = 362 KV, I_D = 69.5 KA, Z_D = 5.2 Ω

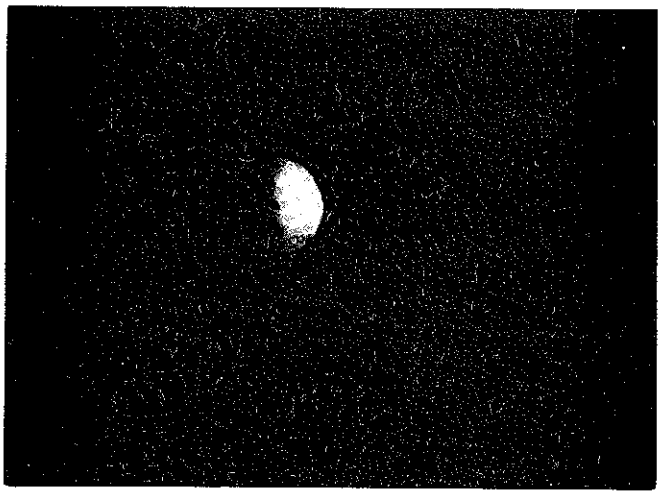

Fig. 11 Time-integrated electron spatial distribution [f/32 + neutral density filter (x 10)].

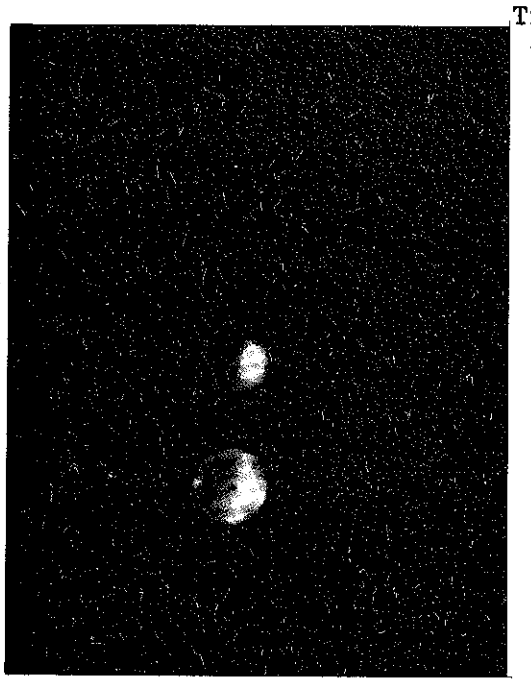

Fig. 12 Time-differentiated electron spatial distribution
5 nsec/frame,
frame separation 50 nsec.
[f/2.0 + neutral density filter (x 40)].

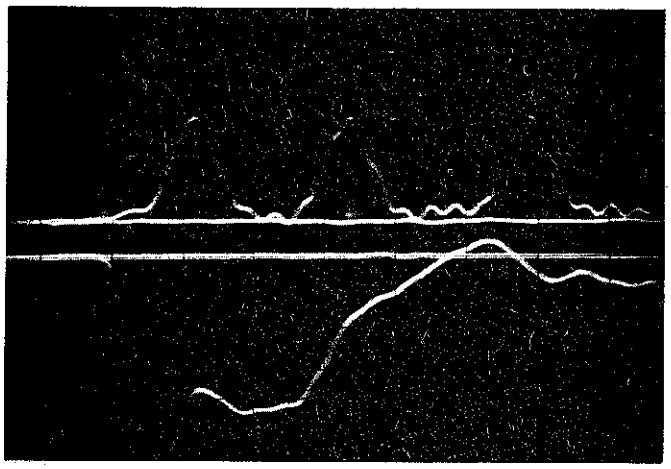

Fig. 13 Lower trace: time-synchronized diode voltage (V_D)

Upper trace: TRW framing camera marking pulses (20nsec./cm)

Unclassified
Security Classification

DOCUMENT CONTROL DATA - R & D

(Security classification of title, body of abstract and indexing annotation must be entered when the overall report is classified)

1. ORIGINATING ACTIVITY *(Corporate author)*

Laboratory of Plasma Studies
Cornell University
Ithaca, New York 14850

2a. REPORT SECURITY CLASSIFICATION

Unclassified

2b. GROUP

--

3. REPORT TITLE

BEAM ENTRANCE CONDITION STUDIES

4. DESCRIPTIVE NOTES *(Type of report and, inclusive dates)*

Topical Research Report

5. AUTHOR(S) *(First name, middle initial, last name)*

John J. Clark
Simpson Linke

6. REPORT DATE	7a. TOTAL NO. OF PAGES	7b. NO. OF REFS
May 1969	21	2

8a. CONTRACT OR GRANT NO.	9a. ORIGINATOR'S REPORT NUMBER(S)
N00014-67-A-0077-0003	LPS 13
b. PROJECT NO.	
c.	9b. OTHER REPORT NO(S) *(Any other numbers that may be assigned this report)*
d.	--

10. DISTRIBUTION STATEMENT

Qualified requestors may obtain copies of this report by writing to Director, Laboratory of Plasma Studies, Upson Hall, Cornell University, Ithaca, NY 14850.

11. SUPPLEMENTARY NOTES	12. SPONSORING MILITARY ACTIVITY
None	Plasma Physics Division Naval Research Laboratory Washington, D.C. 20390

13. ABSTRACT

Observed operational characteristics of the high-field-emission diode of the Cornell Relativistic Electron Beam Accelerator are presented as functions of diode impedance over a range of cathode types, anode-cathode gap spacings, and vacuum pressures. Comparisons are made with expected predictions from the Child-Langmuir Law. Pin-hole, anode-plane radiographs are displayed, for a number of cathode designs, showing spatial current distribution and angular spread of electron trajectories. Preliminary studies of the time history of the current distribution in the anode-cathode gap are described. Results are presented in photographs obtained by fast-frame and time-integrated cameras.

14. KEY WORDS	LINK A		LINK B		LINK C	
	ROLE	WT	ROLE	WT	ROLE	WT
Plasma physics Relativistic Electron Beams High-Field-Emission Diodes Diode Impedance						